Organic “Receptor” Fully Covered Few-layer Organic-metal Chalcogenide for High-Performance Chemiresistive Gas Sensing at Room Temperature

Huijie Jiang,[ab] Linan Cao,[ab] Yanzhou Li,[a] Wenhua Li,[a] Xiaoliang Ye,[a] Weihua Deng,[ab]
Xiaoming Jiang,[a] GuanE. Wang,[a] and Gang Xu*[ab]

[a] State Key Laboratory of Structural Chemistry, Fujian Institute of Research on the Structure of Matter, Chinese Academy of Sciences (CAS),
No. 155 Yangqiao Road West, Fuzhou, Fujian, 350002, P. R. China

[b] University of Chinese Academy of Sciences (UCAS),
No. 19A Yuquan Road, Beijing 100049, P. R. China

Corresponding author: Gang Xu
gxu@fjirsm.ac.cn

Tab. of contents

1. Synthesis of few-layer Ag(SPh-NH_2)

A hydrothermal method was employed to synthesize few-layer Ag(SPh-NH_2). Typically, 15 uL HSPh-NH_2 (4-Aminobenzenethiol) and 7.5 mg silver nitrate were dissolved in 25 and 15 mL DI Water, respectively. Then the solution containing silver nitrate was added to the HSPh-NH_2 solution drop by drop with strong stirring in 5 minutes. After stirring for half an hour, the mixture turned to a transparent yellow solution and then was transferred to a 50 mL glass vial for keeping at 85 ^oC. After 24 hours, homogeneous pale yellow suspension was obtained as the product. The product was collected by centrifugation, and then washed by DI Water and ethanol for 3 times, respectively.

The few-layer Ag(SPh-NH_2) suspension for thin film fabrication was prepared by dispersing the product in ethanol in a concentration of 2mg mL^{-1}.

2. Synthesis of few-layer Ag(SPh)

Typically, 17 mg silver nitrate and 67 mg benzenethiol (HSPh) were dissolved in 40 and 120 mL ethanol, respectively; then the solution containing silver nitrate was dropwisely added to the HSPH solution with strong stirring in 5 minutes. After that, the mixture was kept on stirring at room temperature. After 12 hours, uniform white suspension was obtained as the product. The product was collected by centrifugation, and then washed by ethanol for 3 times. Finally, the solid product was dispersed in ethanol to form a 2 mg mL^{-1} suspension for thin film preparation.

3. Characterizations

Powder X-ray diffraction (PXRD) of samples were recorded on a Rigaku Smartlab X-ray diffractometer with 1D array detector using Cu Kα radiation (λ = 1.54178 Å). The morphology of samples was observed by scanning electron microscope (SEM, JEOL JSM-6700F) and transmission electron microscope (TEM, Tecnai F20). The thickness and size of samples were measured by scanning probe microscope (SPM, Dimension Icon). X-ray photoelectron spectroscopy (XPS) and ultra-violet photoelectron spectroscopy (UPS) were conducted on a Thermo Scientific ESCALAB 250 Xi XPS system. Fourier transform infrared spectroscopy (FTIR) spectra were recorded on a Bruker VERTEX70 FT-IR spectrometer (Germany) in 4000–400 cm^{-1} region using KBr pellets. *In-situ* diffuse reflectance infrared Fourier transform spectroscopy (DRIFTS) experiments were performed on a 6700 Fourier transform-infrared spectrometer (Nicolet) equipped with a stainless steel *in-situ* IR flow cell and set up for diffuse reflectance sampling. UV-vis diffuse reflectance spectra (DRS) were recorded on a Lamda 950 (PerkinElmer, USA) using $BaSO_4$ as a reference. The electrical measurements were performed using a Keithley 4200 (USA) semiconductor characterization system.

4. Fabrication of thin film devices

The thin films were fabricated by conventional spin-coating method. Quartz substrates (2 * 2 cm) used here were washed with DI Water, acetone, ethanol via sonication for 10 minutes, separately; then the substrates were dried by Argon flow and then dried at 100 ^oC. Typically, the sample suspension was dropped on the surface of quartz to fully cover the surface; firstly rotated at low speed of 100 rpm for 20 seconds and followed by high-speed rotation of 2000 rpm for 20 seconds to remove extra suspension; then repeated this process for 10 times successively; finally, all the films were dried at 85 ^oC for one hour. After that, 5 nm Cr and 50 nm Au were deposited on films successively by thermal evaporation (RH 400, Shenyang Pengcheng Vacuum Technology Co. Ltd., China) to form an interdigital electrode with a gap width of 0.5 um.

5. Gas sensing measurements

The sensing property assessment was performed with a home-made system reported in our previous work[1]. The devices were connected to this test system by two Au wires with conductive silver paint. All tests were performed at room temperature. It cost about 40 s to fulfill the chamber of test system when the gas flow was 600 mL min^{-1}. Two mass flow controllers were used to accurately control the flows of the analyte gases and dry air, respectively, to obtain controlled concentrations of the target gases. The constant flow was 600 mL min^{-1}, the bias on the sensor was 5 V and the electrical signal was recorded by using Keithley 2602B Sourcemeter.

6. Calculations of response, response / recovery time and coefficient of variation

The response (R) is defined as: R = ($R_{analyte}$ / R_{air} -1) or R= (R_{air} / $R_{analyte}$ -1), Where R_{air} and $R_{analyte}$ are the resistance of the devices in air and analyte, respectively.

The response time of the sensor is the time required increasing the response to 90% of the saturation value and the recovery time is the time required decreasing the response to its 10%.

The coefficient of variation (CV) is defined as: CV = R_{SD} / $R_{average}$ ×100%, where R_{SD} and $R_{average}$ are the standard deviation (SD) and average value of responses with five successive cycles.

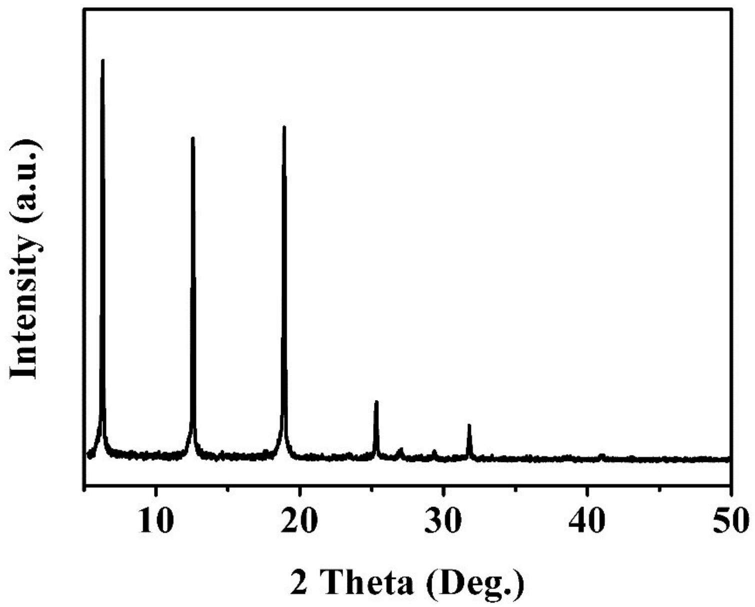

Fig. S1 PXRD pattern of few-layer Ag(SPh).

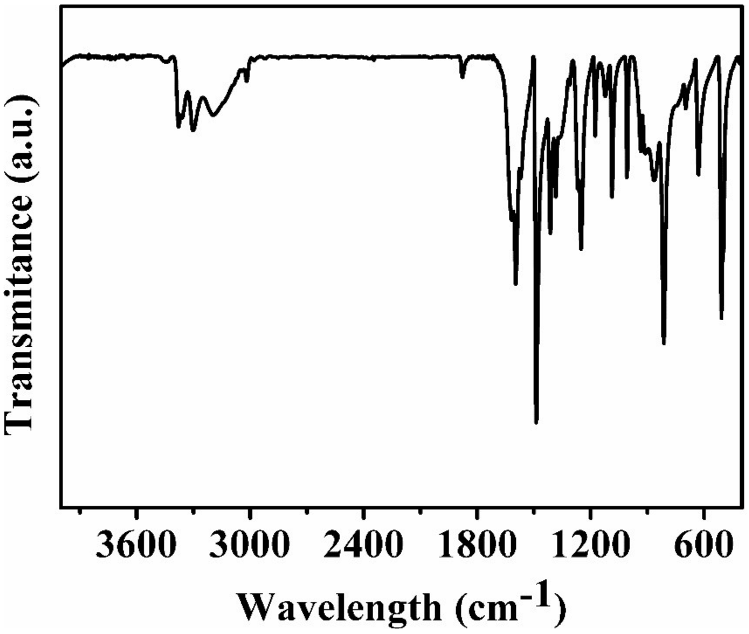

Fig. S2 FTIR spectrum of Ag(SPh-NH_2).

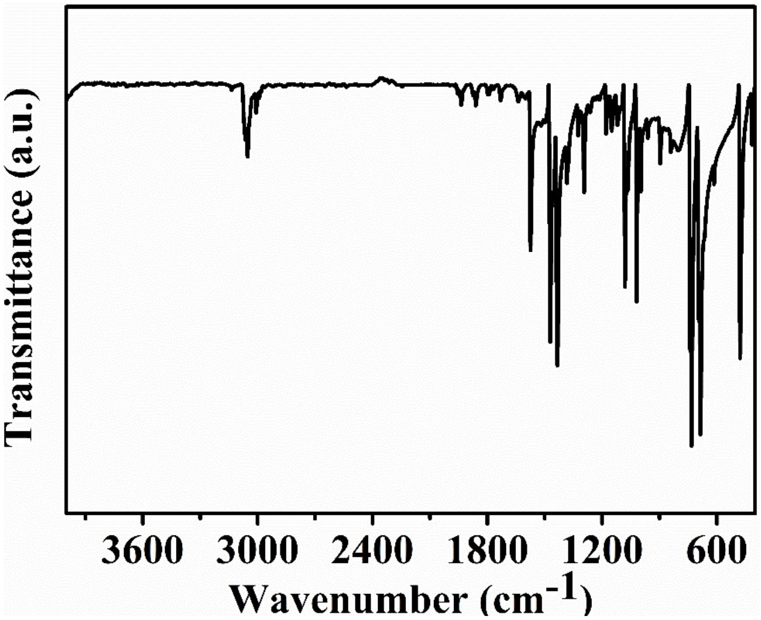

Fig. S3 FTIR spectrum of Ag(SPh).

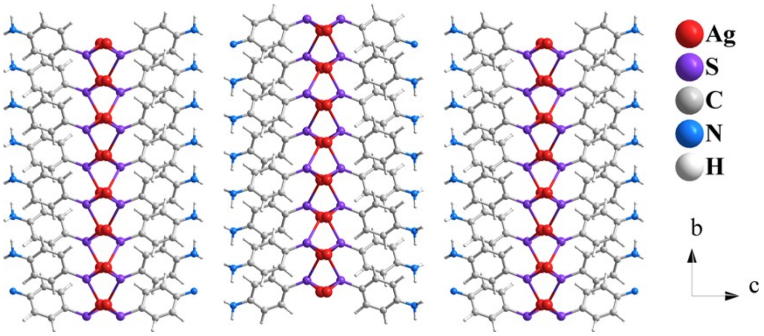

Fig. S4 Packing structure of Ag(SPh-NH$_2$) perpendicular to a direction.

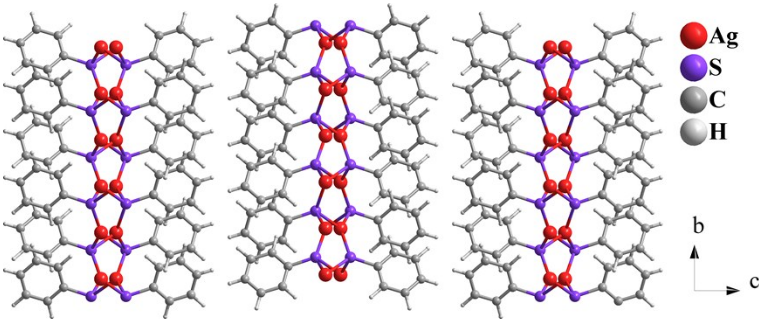

Fig. S5 Packing structure of Ag(SPh) perpendicular to a direction.

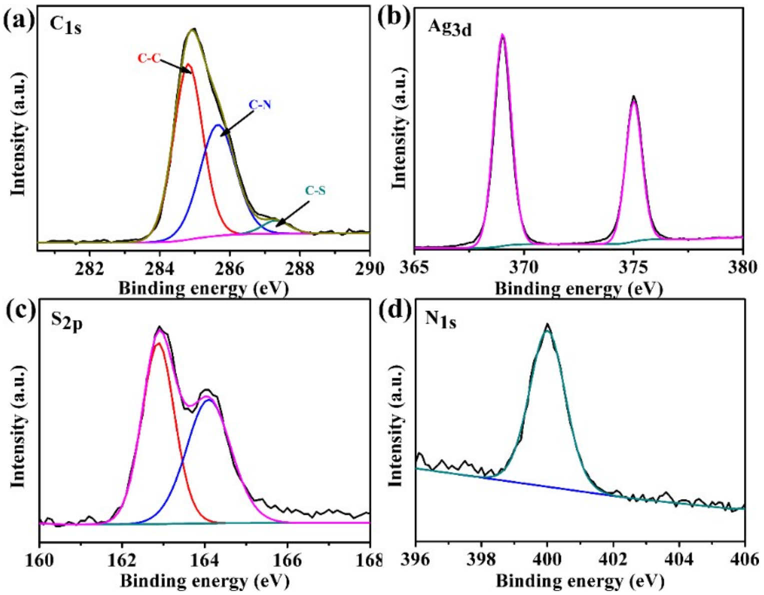

Fig. S6 High-resolution XPS spectrum of C_{1s}, Ag_{3d}, S_{2p}, N_{1s} of Ag(SPh-NH_2).

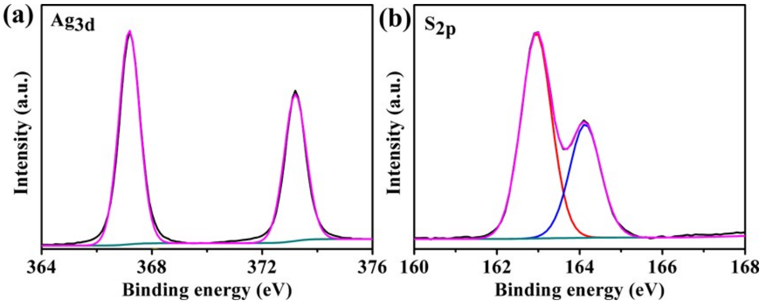

Fig. S7 High-resolution XPS spectrum of Ag_{3d}, S_{2p}, of Ag(SPh).

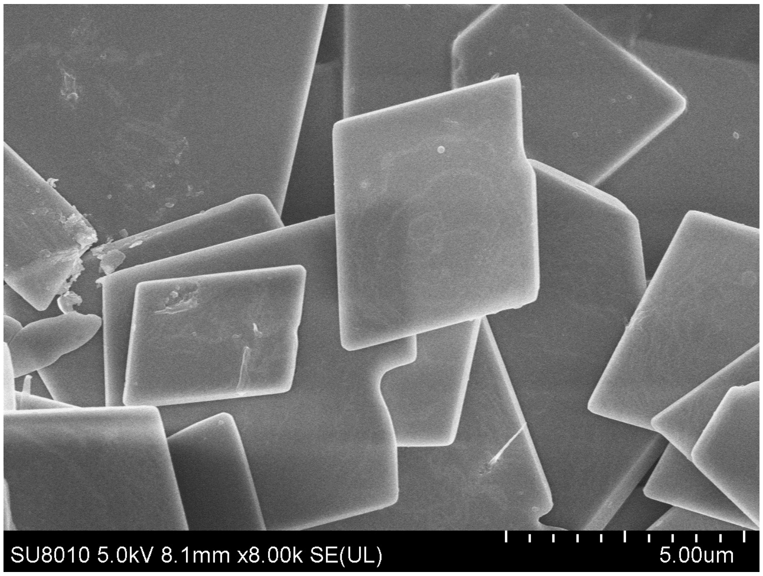

Fig. S8 SEM image of Ag(SPh).

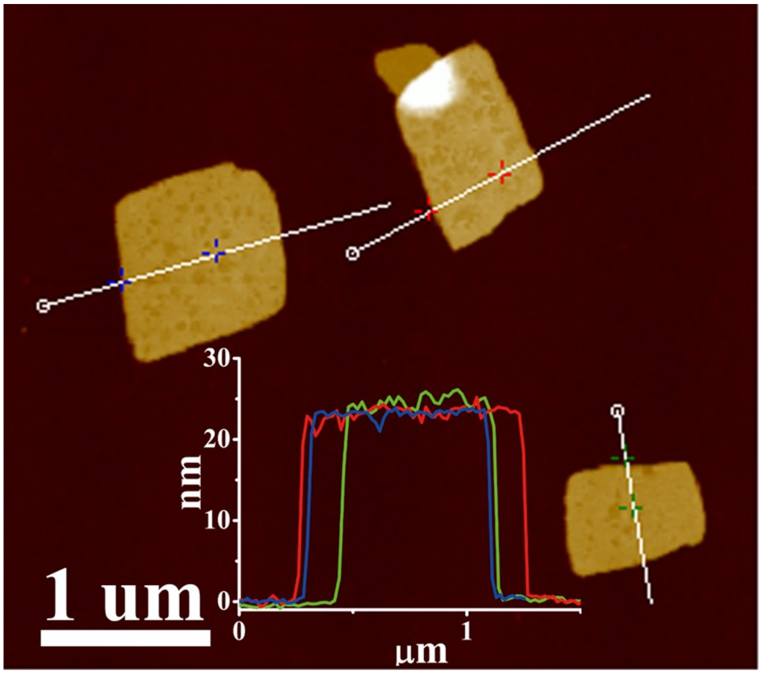

Fig. S9 AFM image of few-layer Ag(SPh).

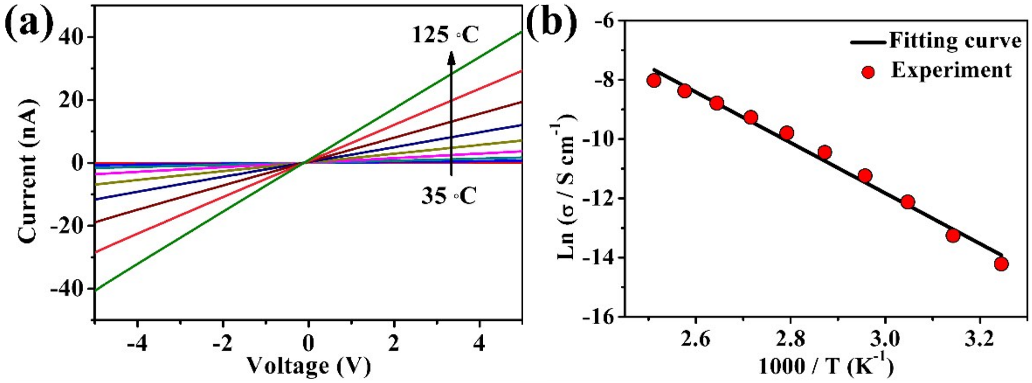

Fig. S10 a) Temperature-dependent I-V curves and b) temperature-dependent conductivity of Ag(SPh-NH$_2$).

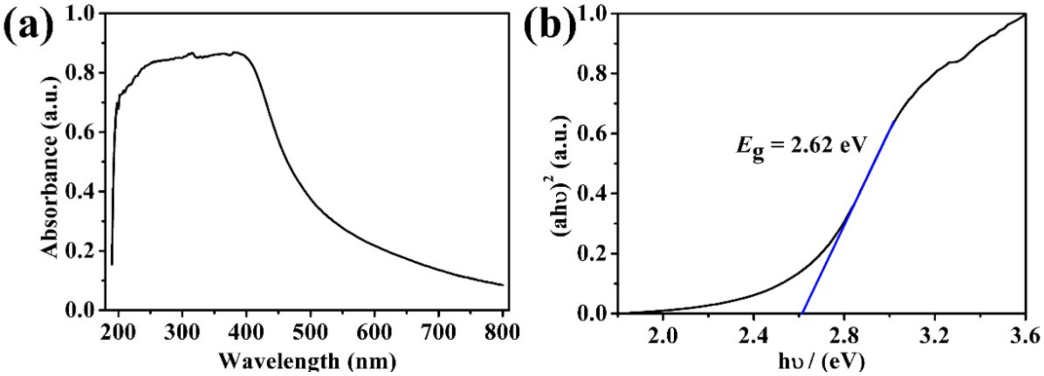

Fig. S11 a) UV-vis DRS and b) optical band gap of Ag(SPh-NH_2).

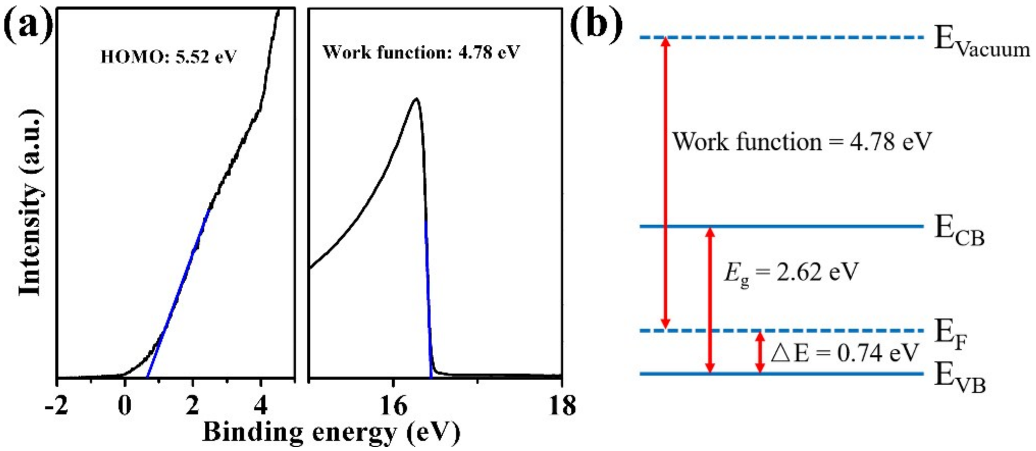

Fig. S12 a) UPS and b) energy band diagram of Ag(SPh-NH_2).

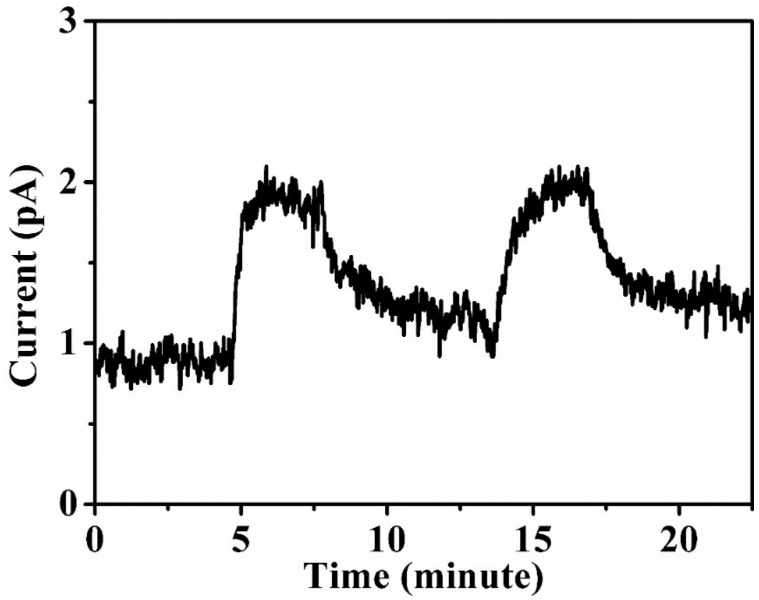

Fig. S13 Response and recovery curve of few-layer Ag(SPh-NH_2) to 0.1 ppm NO_2.

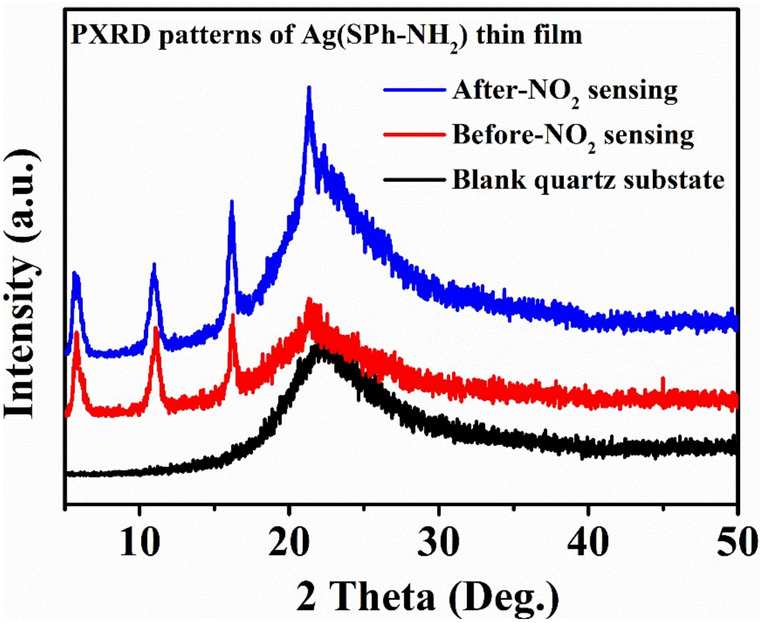

Fig. S14 PXRD patterns of Ag(SPh-NH$_2$) thin film before and after NO2 sensing.

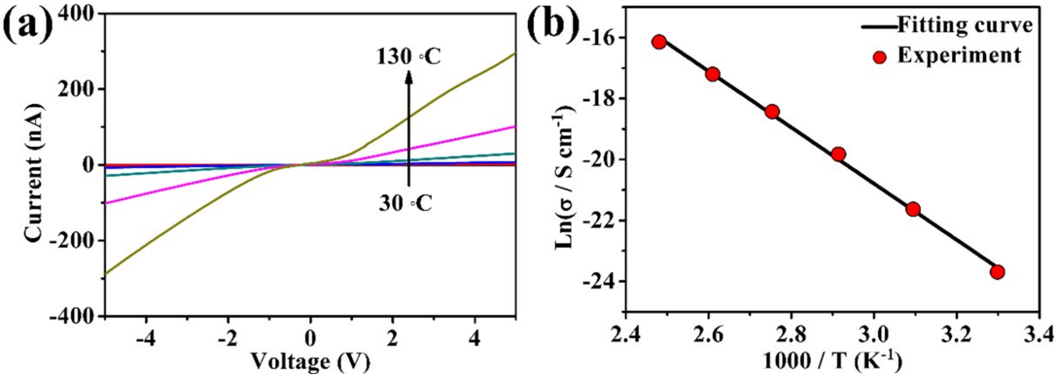

Fig. S15 a) Temperature-dependent I-V curves and b) Temperature-dependent conductivity of Ag(SPh).

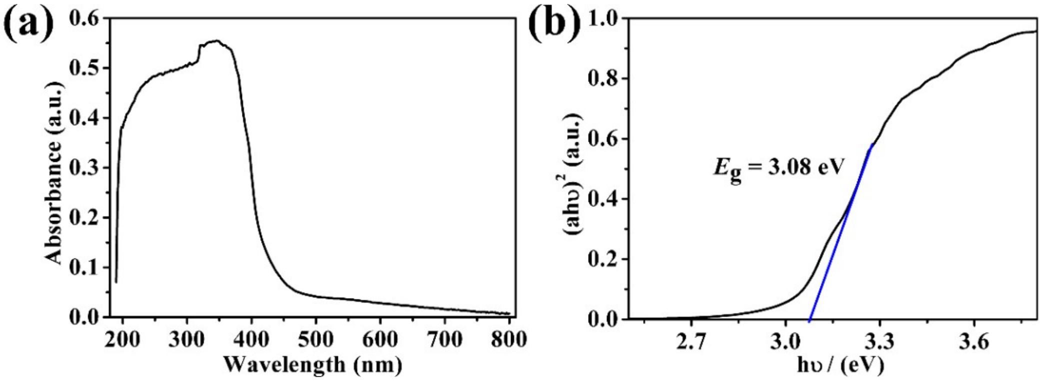

Fig. S16 a) UV-vis DRS) and b) optical band gap of Ag(SPh).

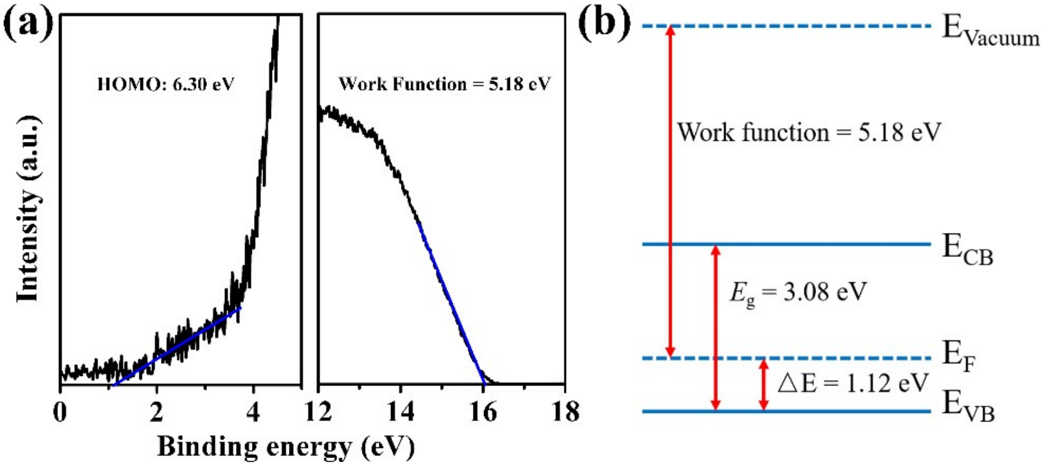

Fig. S17 a) UPS) and b) energy band diagram of Ag(SPh).

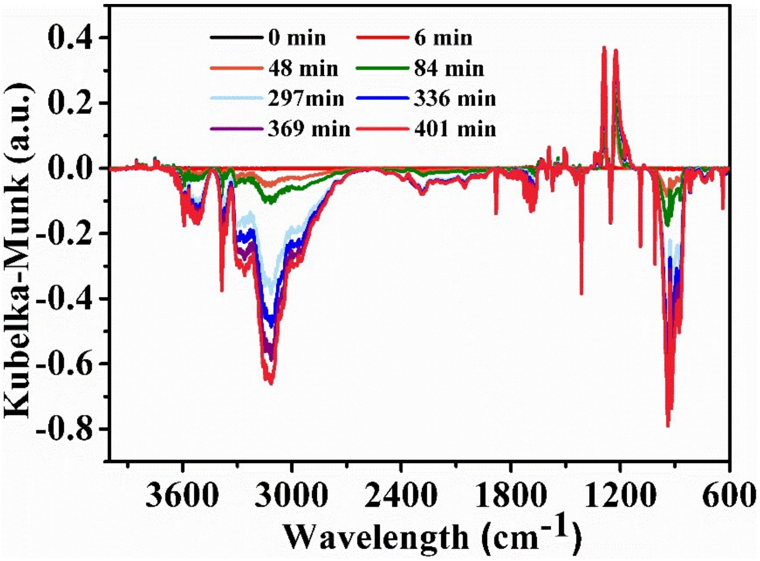

Fig. S18 *In-situ* DRIFTS of Ag(SPh-NH_2) being exposed to NO_2 gas.

Tab. S1 Elemental analysis of Ag(SPh-NH_2) and Ag(SPh).

Compound	C (Theoretical)	C (Experimental)	S (Theoretical)	S (Experimental)	H (Theoretical)	H (Experimental)
Ag(SPh-NH_2)	31.06	29.85	13.82	13.88	2.61	2.52
Ag(SPh)	33.20	32.64	14.77	13.67	2.32	2.01

Tab. S2 Response values of Ag(SPh-NH_2) to 10 ppm NO_2 within five cycles.

cycle	1	2	3	4	5
Response (%)	1080	1097	1084	1053	1034

Tab. S3 Sensing performances of typical 2D material-based RT chemiresistive NO_2 sensor.

Sensing layer	Sensitivity (%)	Response & Recovery time (min)	LOD (ppb)	Ref.
MoS_2	120 @ 1ppm	-/-	120	2
$MoSe_2$	90 @ 100 ppm	5/10	5000	3
WS_2	68 @ 5 ppm	-/-	100	4
NbS_2	18 @ 5 ppm	50/150	240	5
Graphene	25 @ 200 ppm	2/5	-	6
Bilayer Graphene	12.87 @ 5 ppm	-/-	-	7
GO	17 @ 5 ppm	-/-	650	8
RGO	1.5 @ 100 ppm	5/20	-	9
Holey RGO	31.8 @ 3 ppm	-/-	60	10
Ozone treated Graphene	16 @ 200 ppm	15/30	1.3	11
S-G	88 @ 5 ppm	5/30	3600	12

EDA-G	22 @ 1 ppm	10/30	70	12
CFGO	76.3 @ 5 ppm	-/-	-	13
ANS-RGO	95 @ 10 ppm	3.3/23.3	-	14
BP	80 @ 1 ppm	1.2/-	100	15
Ag(SPh-NH_2)	852.6 @ 10 ppm	1.0/2.3	0.9	This work

Tab. S4 Response of Ag(SPh-NH_2) to NO_2 and other interference gases.

Gases	NO_2	SO_2	CO_2	H_2S	EtOH	CO	H_2	CH_4	Benzene	Toluene	NH_3	TEA	Acetone
Con. (ppm)	100	10	100	100	100	100	100	100	100	100	100	100	100
Response	2017	0	6.1	10.1	9.3	7.5	10.5	10.3	11.1	12.7	-8.1	-15	-6.5

References

1 M. S. Yao, W. X. Tang, G. E. Wang, B. Nath and G. Xu, *Adv. Mater.,* 2016, **28**, 5229.

2 B. Cho, A. R. Kim, Y. Park, J. Yoon, Y. J. Lee, S. Lee, T. J. Yoo, C. G. Kang, B. H. Lee, H. C. Ko, D. H. Kim and M. G. Hahm, *ACS Appl. Mater. Inter.,* 2015, **7**, 2952.

3 S. Zhang, T. H. Nguyen, W. Zhang, Y. Park and W. Yang, *Appl. Phys. Lett.,* 2017, **111**, 161603.

4 T. T. Xu, Y. Y. Liu, Y. Y. Pei, Y. P. Chen, Z. M. Jiang, Z. F. Shi, J. M. Xu, D. Wu, Y. T. Tian and X. J. Li, *Sens. Actuators B Chem.,* 2018, **259**, 789.

5 Y. Kim, K. C. Kwon, S. Kang, C. Kim, T. H. Kim, S. P. Hong, S. Y. Park, J. M. Suh, M. J. Choi, S. Han and H. W. Jang, *ACS Sens.,* 2019, **4**, 2395.

6 C. Lee, J. Ahn, K. B. Lee, D. Kim and J. Kim, *Thin Solid Films,* 2012, **520**, 5459.

7 Y. Seekaew, D. Phokharatkul, A. Wisitsoraat and C. Wongchoosuk, *Appl. Surf. Sci.,* 2017, **404**, 357.

8 Y. R. Choi, Y. G. Yoon, K. S. Choi, J. H. Kang, Y. S. Shim, Y. H. Kim, H. J. Chang, J. H. Lee, C. R. Park, S. Y. Kim and H. W. Jang, *Carbon,* 2015, **91**, 178.

9 G. Lu, L. E. Ocola and J. Chen, *Nanotechnology,* 2009, **20**, 445502.

10 D. H. Wang, Y. Hu, J. J. Zhao, L. L. Zeng, X. M. Tao and W. Chen, *J. Mater. Chem. A,* 2014, **2**, 17415.

11 M. G. Chung, D. H. Kim, H. M. Lee, T. Kim, J. H. Choi, D. K. Seo, J. B. Yoo, S. H. Hong, T. J. Kang, and Y. H. Kim, *Sens. Actuators B Chem.,* 2012, **166**, 172.

12 W. Yuan, A. Liu, L. Huang, C. Li and G. Shi, *Adv. Mater.,* 2013, **25**, 766.

13 Y. H. Kim, J. S. Park, Y. R. Choi, S. Y. Park, S. Y. Lee, W. Sohn, Y. S. Shim, J. H. Lee, C. R. Park, Y. S. Choi, B. H. Hong, J. H. Lee, W. H. Lee, D. Lee and H. W. Jang, *J. Mater. Chem. A,* 2017, **5**, 19116.

14 W. L. Pei, T. T. Zhang, Y. Wang, Z. Chen, A. Umar, H. Li and W. Guo, *Nanoscale,* 2017, **9**, 16273.

15 S. Y. Cho, Y. Lee, H. J. Koh, H. Jung, J. S. Kim, H. W. Yoo, J. Kim and H. T. Jung, *Adv. Mater.,* 2016, **28**, 7020.